

Nanoscale

Accepted Manuscript



This is an *Accepted Manuscript*, which has been through the Royal Society of Chemistry peer review process and has been accepted for publication.

Accepted Manuscripts are published online shortly after acceptance, before technical editing, formatting and proof reading. Using this free service, authors can make their results available to the community, in citable form, before we publish the edited article. We will replace this *Accepted Manuscript* with the edited and formatted *Advance Article* as soon as it is available.

You can find more information about *Accepted Manuscripts* in the [Information for Authors](#).

Please note that technical editing may introduce minor changes to the text and/or graphics, which may alter content. The journal's standard [Terms & Conditions](#) and the [Ethical guidelines](#) still apply. In no event shall the Royal Society of Chemistry be held responsible for any errors or omissions in this *Accepted Manuscript* or any consequences arising from the use of any information it contains.



Co-delivery of doxorubicin and arsenite with reduction and pH dual-sensitive vesicle for synergistic cancer therapy

Lu Zhang,^{a†} Hong Xiao,^{a†} Jingguo Li,^a Du Cheng,^{*a} Xintao Shuai^{†*a,b}

Received 00th January 20xx,
Accepted 00th January 20xx

DOI: 10.1039/x0xx00000x

www.rsc.org/

Drug resistance is the underlying cause for therapeutic failure in clinical cancer chemotherapy. A prodrug copolymer mPEG-PAsp(DIP-co-BZA-co-DOX) (PDBD) was synthesized and assembled into nanoscale vesicle comprising a PEG corona, a reduction and pH dual-sensitive hydrophobic membrane and an aqueous lumen encapsulating doxorubicin hydrochloride (DOX·HCl) and arsenite. The dual stimulation-sensitive design of vesicle gave rise to rapid release of the physically entrapped DOX·HCl and arsenite inside acidic lysosomes, and chemically conjugated DOX inside cytosol with high glutathione (GSH) concentration. At optimized concentration range, arsenite (As) previously recognized as a promising anticancer agent from traditional Chinese medicine can down-regulate the expressions of anti-apoptotic and multidrug resistance proteins to sensitize cancer cells to chemotherapy. Consequently, the DOX-As-loaded vesicle demonstrated potent anticancer activity. Compared to the only DOX-loaded vesicle, the DOX-As-co-loaded one induced more than twice the apoptotic ratio of MCF-7/ADR breast cancer cells at the low As concentration (0.5 μM), due to the synergistic effects of DOX and As. The drug loading strategy integrating chemical conjugation and physical encapsulation in stimulation-sensitive carrier enabled efficient drug loading in the formulation.

Introduction

Chemotherapy is one of the three major means for clinic cancer treatment. Yet, it is facing tremendous challenges in treating almost all types of cancers, and chief among them are the drug resistance of cancer cells and systemic side effects which damage healthy cells and tissues. Recent advances have shown that the situation may be

improved by using polymeric nanocarriers to deliver the anticancer drugs. Polymeric nanomedicines are apt to accumulate in tumor sites *via* mechanism known as enhanced permeability and retention (EPR) effect.¹⁻⁵ Moreover, it is reported that nanocarriers could overcome drug resistance by circumventing the drug efflux pumps such as P-glycoprotein (P-gp).⁶⁻⁹

It is well-known that there are two strategies to incorporate anticancer drugs into polymeric nanocarriers. The first one is the physical encapsulation, which represents the majority of polymeric nanomedicines. In this event, amphiphilic block copolymers are assembled into micellar or vesicular structures. The hydrophobic micelle core or vesicle membrane can encapsulate hydrophobic drugs *via* hydrophobic interaction, whereas the aqueous lumen of vesicles can provide accommodation for hydrophilic drugs. This strategy is easy to implement and versatile for encapsulation of various drugs. However, the drug loading contents *via* physical entrapment are generally low and drugs may leak out of

^a PCFM and GDHPPC labs, School of Chemistry and Chemical Engineering, Sun Yat-sen University, Guangzhou 510275, China

^b Center of Biomedical Engineering, Zhongshan School of Medicine, Sun Yat-sen University, Guangzhou 510080, China

†These authors contributed equally to this work.

*Correspondence should be addressed to:

Xintao Shuai

Tel.: +86-20-84110365

Fax: +86-20-84112245;

E-mail: shuaixt@mail.sysu.edu.cn

Du Cheng

Tel.: +86-20-84112172; Fax: +86-20-84112245.

E-mail: chengdu@mail.sysu.edu.cn

Electronic Supplementary Information (ESI) available: [details of any supplementary information available should be included here]. See DOI: 10.1039/x0xx00000x

ARTICLE

nanomedicines in blood circulation.^{10, 11} In contrast, the second approach adopts chemical conjugation to load drugs into polymeric nanocarriers, which decreases the use of carrier materials and meanwhile increases drug loading capacity.^{12, 13} Owing to the chemical conjugation, the nanomedicines are drug leakage-free in blood circulation. To enable release inside tumors, drugs are usually conjugated *via* special linkages which may cleave inside tumor tissues or cells.¹⁴⁻¹⁷ For example, utilizing the concentration difference of a reducing agent glutathione (GSH) in bloodstream (<5 μM) and cytosol of cancer cells (up to millimolar scale), drugs conjugated through disulfide bonds will not leak in blood circulation but will quickly release from the nanocarriers inside cancer cells.¹⁸⁻²¹ Nevertheless, a big limitation exists as chemical conjugation requires drugs to possess at least one reactive site, which is unfortunately not available for many anticancer drugs. At present, it is still of great importance to optimize drug encapsulation *via* a microenvironment-sensitive design (e.g. pH or reduction sensitive) for tumor-specific drug release as well as to integrate physical entrapment and chemical conjugation for combined advantages.

On the other hand, drug resistance is known as the major underlying cause for chemotherapy failure. Many studies have demonstrated that drug resistance in cancer chemotherapy was generally resulted from the over-expressions of anti-apoptosis proteins such as Bcl-2 and drug efflux proteins such as MDR1 P-glycoprotein (P-gp), which significantly decreased the sensitivity of cancer cells to chemotherapeutic agents.^{22, 23} Therefore, strategies to overcome chemoresistance of cancer cells rely, to a great extent, on the suppression of these proteins' expression. A typical means utilizes the RNA interference (RNAi) technique to silence drug resistance genes in various tumor models, which has been based on the potent target gene silencing of small interference RNA (siRNA).²⁴⁻²⁹ To boost the synergistic effects, siRNA and anticancer drugs should be co-encapsulated inside the same nanocarrier for concurrent delivery. However, due to the distinct natures of the two therapeutic agents, it has been always challenging to prepare a nanocarrier for efficient co-encapsulation and co-delivery.³⁰ Moreover, the issue about therapeutic efficiency is often complicated due to the off-target effect of siRNA.³¹ Therefore, it appears meaningful to search for other easily manipulable alternatives to siRNA for the purpose of reversing drug resistance in tumor chemotherapy. At the optimized concentration range, arsenite previously recognized as a successful anticancer agent for

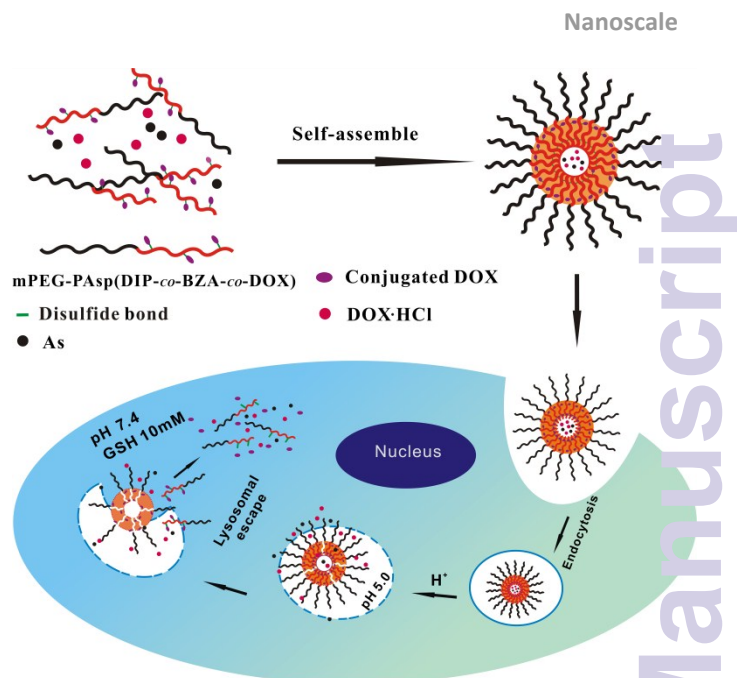


Fig. 1. Schematic illustration of the vesicle preparation and dual-sensitive release of DOX and arsenite inside cancer cells.

acute promyelocytic leukemia (APL) therapy was found to suppress drug resistance of cancer cells through multiple mechanisms including down-regulation of the Bcl-2 and P-gp proteins,³²⁻³⁴ which enlightened us to consider whether the tumours expressing high levels of Bcl-2 and P-gp proteins may be re-sensitized to chemotherapy *via* a concurrent arsenite treatment.

Herein, we describe a novel reduction and pH dual-sensitive vesicle carrying arsenite and doxorubicin (DOX) for a combined anticancer therapy (Fig. 1). DOX was loaded into the vesicle by both physical entrapment and chemical conjugation, in order to integrate the advantages of the two drug encapsulation strategies, e.g. to improve DOX loading. The dual-sensitive structural design was expected to allow the vesicle to quickly release its cargos in response to the intracellular microenvironments of cancer cells (Fig. 1). In addition, the two co-delivered therapeutic agents were expected to exert synergistic anticancer effects, i.e. DOX resistance of cancer cells might be suppressed by arsenite *via* downregulating the Bcl-2 expression.

Experimental

Materials

ϵ -Benzylloxycarbonyl *L*-aspartic acid NCA (BLA-NCA) was synthesized as reported.³⁵ α -Methoxy- ϵ -hydroxy-poly(ethylene

glycol) (mPEG-OH, Mn=2 kDa, Fluka) was converted to α -methoxy- ϵ -amino poly(ethylene glycol) (mPEG-NH₂) according to the literature.³⁶ *N,N*-dimethylformamide (DMF, 99.8%, Alfa Aesar) was used as received. Dimethylsulfoxide (DMSO, Sigma-Aldrich) was dried over CaH₂ and then distilled. All solvents were of analytical grade. *N,N*-Diisopropylethylenediamine (DIP, 97%, J&K), 2-Mercaptoethylamine (MEA, Sigma-Aldrich), 2, 2'-dipyridyl disulfide (98%, J&K), triethylamine (TEA, Sigma-Aldrich), benzylamine (BZA, Sigma-Aldrich), *N*-Succinimidyl S-acetylthioacetate (SATA, Pierce, Rockford, Illinois), 3-(4,5-dimethyl-thiazol-2-yl)-2,5-diphenyl tetrazolium bromide (MTT, Sigma-Aldrich), doxorubicin hydrochloride (DOX·HCl, Zhejiang Hisun, Pharmaceutical Co., Ltd., China), dithiothreitol (DTT, Acros Organics) were used as received. Dialysis tubes (MWCO: 1, 3.5, 7, 14 kDa) were purchased from Shanghai Green Bird Technology Development Co., Ltd., China. Cell lines were purchased from Bogoo Biotechnology Corporation (Shanghai, China). Cell culture medium, 0.25% trypsin-EDTA, PBS and fetal bovine serum (FBS) were purchased from Life Corporation (Gibco, USA).

Synthesis of poly(ethylene glycol)-*b*-poly(β -benzyl-L-aspartate) (mPEG-PBLA)

mPEG-PBLA was synthesized by ring-opening polymerization of BLA-NCA using mPEG-NH₂ as a macroinitiator. Briefly, under an argon atmosphere, BLA-NCA (4.5 g) was dissolved in 3 mL of anhydrous DMF, and mPEG-NH₂ (0.6 g) was dissolved in 18 mL of anhydrous dichloromethane. The two solutions were mixed by magnetic stirring. The polymerization was performed at 35 °C for 72 h. The solution was concentrated by rotary evaporation, precipitated into cold ether, filtrated, and vacuum-dried to get mPEG-PBLA (yield: 86.2%).

Synthesis of poly(ethylene glycol)-*b*-poly(2-(diisopropylamino)ethyl aspartate-co-benzylamineaspartate) (mPEG-PAsp(DIP-co-BZA))

126 mg BZA and 4 g mPEG-PBLA were added to 25 mL anhydrous DMSO in a reaction vial under argon. The solution was magnetically stirred for 24 h at 35 °C, and then 1.81 g DIP dissolved in 5 mL anhydrous DMSO was added. The reaction was further conducted for 24 h, and the solution was dialyzed (MWCO: 3.5 kDa) against methanol for 72 h under argon and dried by rotary evaporation to get mPEG-PAsp(DIP-co-BZA) (yield: 81.2%).

Synthesis of poly(ethylene glycol)-*b*-poly(2-(diisopropylamino)ethyl aspartate-co-benzylamineaspartate-co-2-(2-pyridinyldithio)ethylamineaspartate) (mPEG-PAsp(DIP-co-BZA-co-PDTA))

To prepare mPEG-PAsp(DIP-co-BZA-co-MEA), 3 g mPEG-PAsp(DIP-co-BZA) and 117 mg MEA were dissolved in 15 mL anhydrous DMSO under argon, and then the solution was stirred for 48 h at 35 °C. After 2, 2'-Dipyridyl disulfide (1.5 molar equivalent to MEA) in anhydrous DMSO (15 mL) was added, the reaction was allowed to proceed for 24 h under argon at room temperature. The solution was dialyzed (MWCO: 3.5 kDa) against methanol for 72 h under argon, and finally dried by rotary evaporation to get mPEG-PAsp(DIP-co-BZA-co-PDTA) (yield: 92.3%).

Synthesis of thiolated doxorubicin (DOX-SH)

DOX-SH was obtained as reported previously.¹⁶ Briefly, 72 mg SATA was dissolved in 5 mL of DMSO and DOX·HCl (17 mg) was dissolved in 600 μ L PBS. The two solutions were magnetically stirred at room temperature. After 0.5 M hydroxylamine (NH₂OH) was added, 6.8 mL of PBS (pH 7.4) supplemented with 25 mM EDTA was added, the reaction was performed for 2 h under nitrogen and away from light to get DOX-SH (yield 91.7%).

Synthesis of poly(ethylene glycol)-*b*-poly(2-(diisopropylamino)ethyl aspartate-co-benzylamineaspartate-co-doxorubicinaspartate) (mPEG-PAsp(DIP-co-BZA-co-DOX))

In a reaction vial under nitrogen protection, 0.4 g mPEG-PAsp(DIP-co-BZA-co-PDTA) was dissolved in 15 mL anhydrous DMSO, and then DOX-SH was added to the solution. The mixture was sealed off under argon and then stirred for 48 h away from light. After reaction, the solution was dialyzed (MWCO: 3.5 kDa) for 48 h against methanol to remove DMSO and excessive DOX-SH, and finally dried by rotary evaporation to get mPEG-PAsp(DIP-co-BZA-co-DOX) (yield: 85.6%).

Characterization

The transmission electron microscopy (TEM) observation of vesicles was performed using a Philips CM120 transmission electron microscope (Philips, Eindhoven, The Netherlands) operated at 100 kV. A drop of the sample solution (10 μ L, 0.5 mg/mL) was dropped on a copper grid coated with amorphous carbon. A small drop of uranyl acetate solution (2 wt% in water) was applied to the copper

ARTICLE

Nanoscale

grid for staining the sample, and then blotted off with filter paper after 1 min. The grid was finally dried overnight before TEM observation. ^1H NMR spectra was performed using a Varian Unity 300 MHz spectrometer or a Bruker 400 MHz spectrometer and $\text{DMSO-}d_6$ was used as the solvent. The molecular weight distribution of polymer was analyzed using a gel permeation chromatography (GPC) system consisting of a Waters 1515 pump, an Ultrahydrogel TM 500 column, an Ultrahydrogel TM 250 column, and a Waters 2417 differential refractive index detector with PEG as a calibration standard. DMF containing LiBr (1.0 g/L) was used as an eluent at a flow rate of 1.0 mL/min. Raman spectroscopy was collected using a Renishaw Invia Raman Spectrometer with excitation wavelength at 785 nm. The hydrodynamic sizes of vesicles were determined *via* dynamic light scattering (DLS) at 25°C using a 90 Plus/BI-MAS equipment (Brookhaven Instruments Corporation, USA). The particle size was collected on an auto-correlator with a detection angle of scattered light at 90° and 15°, respectively. For each sample, the data from three measurements were averaged to obtain the mean \pm standard deviation (SD).

Preparation of vesicles and physical encapsulation of DOX and As

DOX-As-co-loaded vesicle (D-As-PDBD vesicle) was prepared by the double emulsion method.³⁷ In brief, 5 mg As_2O_3 was dissolved in 0.5 mL NaOH (1 mol/L) solution, and then the solution pH was adjusted to 7.4 by adding HCl (0.5 mol/L) aqueous solution,²² which was used as arsenite aqueous solution. 20 mg mPEG-PAsp(DIP-*co*-BZA-*co*-DOX) was dissolved in 0.4 mL DMSO, and then mixed with 2 mL chloroform. 0.2 mL aqueous solution of DOX·HCl (2 mg) and arsenite (2 mg) was emulsified in the copolymer solution by sonication on ice using a probe sonicator. The primary emulsion was then emulsified by sonication on ice in 10 mL of PBS (pH 7.4, 0.05 mol/L). After five minutes, chloroform was evaporated using a rotary evaporator. The precipitate was dialyzed (MWCO: 14 kDa) against PBS of pH 7.4 to remove free DOX·HCl and DMSO. Finally, the vesicle solution was filtered through a 0.45 μm filter membrane to remove large aggregates. Vesicle without physical encapsulation of DOX and As (PDBD vesicle) and vesicle encapsulating hydrophilic DOX but no As (D-PDBD vesicle) were prepared by the same method except drugs added into the aqueous solutions were varied. That is, DOX·HCl (2 mg) and arsenite (2 mg) were not added for the preparation of PDBD vesicle, and DOX·HCl but no arsenite was added for the preparation of D-PDBD vesicle.

Loading contents of DOX and As

The loading content of physically encapsulated DOX was measured using a Unico UV-2000 UV-vis spectrophotometer (Shanghai, China). The freeze-dried D-As-PDBD vesicle was incubated in PBS of pH 5.0 plus 10 mM GSH for 3 days. The absorbance of DOX at 480 nm was measured to determine DOX content in the solution of D-As-PDBD vesicle using a previously established calibration curve. The weight percentage of chemically conjugated DOX in the PDBD vesicle was determined *via* calculating the integral values of characteristic peaks detected by ^1H NMR measurements. The arsenite ion-loading content was measured using Atomic Fluorescence Spectrometer (AFS-2202A, Shanghai Fairburn, China). The determination was conducted in 10% HCl solution, with argon gas used as carrier gas, HCl solution used as current-carrying solution and sodium borohydride-sodium hydroxide (0.2% - 0.5%) solution used as reducing agent. Based on a previously established calibration curve, arsenite atomic fluorescence intensity was measured and then converted to arsenite ion content in the solution.

Stimulation sensitivity of PDBD vesicle and D-As-PDBD vesicle

Vesicle solutions (1 mL each) were incubated for 2 h at different conditions as follows: pH 7.4, pH 5.0, pH 7.4 + 10 mM GSH and pH 5.0 + 10 mM GSH. Then each solution was diluted to 5 mL with an aqueous solution of the same pH value. The fluorescence spectrum of DOX was measured using a PerkinElmer PE-LS55 fluorescence spectrometer (Waltham, USA). An excitation wavelength of 485 nm was used, and the emission spectrum was recorded from 500 to 750 nm with a band width of 10 nm.

In Vitro DOX and Arsenite release from vesicle

Drug release was performed at two pH values (pH 7.4 and 5.0) in the presence or absence of 10 mM GSH. 20 mg PDBD vesicles or D-As-PDBD vesicles was dissolved in 5 mL PBS and then transferred into a dialysis bag (MWCO: 14 kDa) to dialyze against 30 mL of the same PBS at 37 °C in an incubator shaker. At certain time interval, 5 mL of solution outside the dialysis bag was taken for UV-vis analysis and replaced with the same volume of fresh buffer solution. DOX concentration was calculated based on the absorbance intensity of DOX at 485 nm. The concentration of arsenite was measured on an Atomic Fluorescence Spectrometer. The cumulative amount of released drug was calculated using pre-established calibration curves.

and the percentages of drug released from vesicles were plotted against time.

Confocal laser scanning microscopy (CLSM)

The cellular uptake of D-PDBD vesicle and free DOX in MCF-7 cells and MCF-7/ADR cells were observed using confocal laser scanning microscopy (CarlZeiss LSM 710). 1×10^3 cells were incubated overnight in confocal dish at 37 °C. After incubation with D-PDBD or free DOX (DOX concentration: 10 µg/mL) for different time, the cells were washed twice with PBS, and then stained with DAPI solution (1 µg/mL) for 15 min for CLSM observation. Excitations: 485 nm for DOX and 358 nm for DAPI; Emissions: 590 nm for DOX and 455 nm for DAPI.

Cell viability assay

MCF-7 and MCF-7/ADR cells were cultured in DMEM and RPMI-1640 medium containing 10% fetal bovine serum (FBS) under a humidified atmosphere of 5% CO₂ at 37 °C, respectively. The cells were seeded into 96-well plates at a density of 1×10^3 cells per well. After incubation overnight at 37 °C, the cells were incubated with free DOX, free As, D-PDBD vesicle, D-PDBD vesicle plus free As, and D-As-PDBD vesicle at various concentrations for 48 h, and measured with MTT assay. After discarding the old medium, 100 µL fresh medium containing 10 µL MTT solutions (5 mg/mL in PBS) was added into each well to incubate the cells for additional 4 h at 37 °C. Then, 100 µL DMSO was used to replace the above solution and to dissolve the substrate. The absorbance of each well at 570 nm was detected using a Tecan Infinite F200. All experiments were conducted in triplicate.

Cell apoptosis

The MCF-7/ADR cells were seeded into 12-well plates at a density of 1×10^4 cells per well, and then cultured overnight at 37 °C. After incubation with different samples for 48 h, the cells were harvested for cell apoptosis assay. The cells were detached with 0.25% trypsin, collected into EP tubes, washed twice with fresh PBS, and re-suspended in 500 µL binding buffer. 5 µL Annexin V-FITC and 5 µL DAPI solutions were added into the cell suspension which was then incubated for 15 min at room temperature. A Gallios flow cytometry from Beckman Coulter was used to evaluate the cell apoptosis rates. Excitations: 488 nm for Annexin V-FITC and 358 nm for DAPI; Emissions: 530 nm for Annexin V-FITC and 455 nm

for DAPI.

The cell apoptosis rates in different treatment groups were also detected with TUNEL assay. MCF-7/ADR cells were seeded into 24-well plates at a density of 1×10^4 cells per well and cultured overnight. And the cells were incubated with different treatment samples for 48 h. In Situ Cell Death Detection Kit (Roche, Germany) was performed to estimate the percentage of apoptotic cells according to the manufacturer's protocol. In brief, the cells were fixed with 250 µL of 4% paraformaldehyde for 1 h at room temperature and then washed three times with PBS. Afterwards, the cells were blocked with 250 µL of 3% H₂O₂/CH₃OH solution for 15 min at room temperature. After being washed three times with PBS, the cells were permeabilized with 250 µL of 0.1% Triton-X 100 and 0.1% sodium citrate solutions for 2 min on ice. The cells were washed with PBS, treated with 50 µL of TUNEL reaction mixture for 1 h, and incubated with 50 µL of POD for 30 min at 37 °C in a humidified chamber in the dark. The cells were washed with PBS and then treated with 100 µL DAB solution before being observed using an inverted fluorescence microscope (CarlZeiss, Germany).

Real-time PCR

The real-time PCR assay was used to evaluate the mRNA levels of the P-gp and Bcl-2 genes. The MCF-7/ADR cells seeded into 6-well plates were cultured overnight. After incubation with different treatment samples for 48 h, the cells were collected and the total RNA was extracted using the TRIzol reagent Kit (Invitrogen). The first strand cDNA was synthesized using PrimeScript™ RT reagent Kit (Takara, Japan). The quantitative RT-PCR was performed using a FastStart Universal SYBR Green Master (ROX) (Roche, Swiss). The forward and reverse primers sequences of the Bcl-2 gene were 5'-AGTACCTGAACCGGCACCT-3' and 5'-GCCGTACAGTTCCACAAAGG-3', respectively. And the forward and reverse primers sequences of the P-gp gene were 5'-TCCAAGCATTGAAGCATTG-3' and 5'-TCTGGTTTGTGCCCACTCTT-3', respectively. The mRNA level of the β-actin gene as a reference gene was used for normalization of the expression level of mRNA in each sample. The forward primer sequence was 5'-GTACGCCAACACAGTGCTGTCT-3' and the reverse primer sequence was 5'-TGCATCCTGTCCGCAATG-3'. The PCR reaction procedure was as follows: GoldTaq Hot Start Polymerase activation at 95 °C for 10 min, denaturation at 95 °C for 30 s, annealing and extension at 60 °C for 60 s for 40 cycles with a

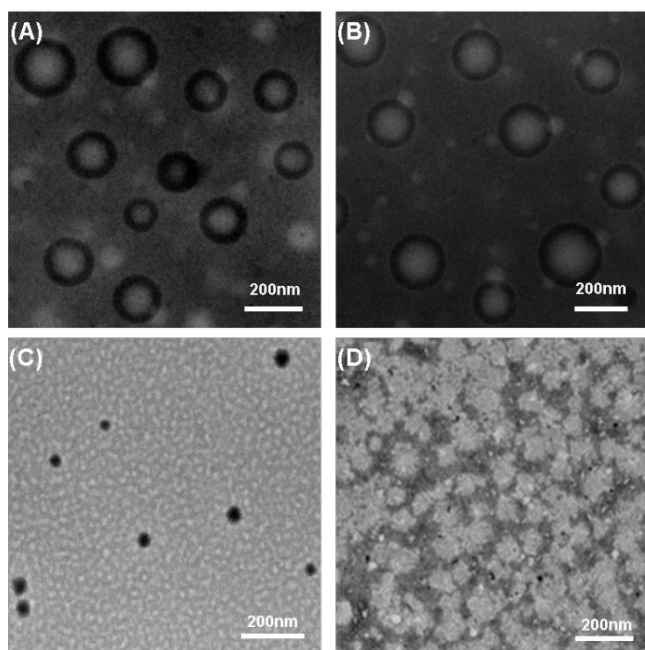


Fig. 2. Transmission electron microscopy (TEM) images of DOX-As-co-loaded vesicle (D-As-PDBD vesicle) at pH 7.4 (A), pH 7.4+GSH (B), pH 5.0 (C) and pH 5.0+GSH (D). (GSH concentration if applied: 10 mM)

Table 1. Size changes of the vesicles measured by DLS.

Sample name	PDBD vesicle		D-As-PDBD vesicle			
	pH 7.4	pH 7.4	pH 7.4	pH 7.4 +GSH ^{a)}	pH 5.0	pH 5.0 +GSH ^{a)}
Size (nm)	173 ±4	179 ±6	182 ±5	210 ±7	35 ±2	ND ^{b)}

^{a)} GSH concentrations if applied: 10 mM; ^{b)} not detected.

StepOne plus Real-time PCR System (ABI, USA). All experiments were conducted in triplicate.

Cell immunofluorescence assay

The expression levels of P-gp proteins and Bcl-2 proteins were estimated with cell immunofluorescence assay. The MCF-7/ADR cells were grown overnight in a 6-well plates and then incubated with different treatment groups. The cells were fixed with 4% paraformaldehyde in PBS for 20 min, washed with PBS, permeated with 0.1% Triton X-100 for 10 min, blocked with 5% BSA in PBS for 1 h, and incubated in primary antibody dilution buffer with 1:100 the primary antibody overnight at 4 °C. The cells were washed with PBS, incubated with secondary antibody goat-anti-rabbit-FITC (1:1000) for 1 h at 37 °C, washed with PBS again, incubated with DAPI (1 µg/mL in PBS) for 15 min, covered with glycerin, and finally observed under a CarlZeiss LSM710 confocal laser scanning microscope.

Results and discussion

Polymer synthesis and vesicle preparation

The reduction and pH dual-sensitive block copolymer mPFG-PAsp(DIP-co-BZA-co-DOX) (PDBD) for the formation of dual-sensitive vesicle was synthesized by multistep chemical reactions as outlined in Fig. S1. The hydrophobic block of the copolymer consisted of poly(L-aspartic acid) randomly grafting (diisopropylamino)ethylamine (DIP), benzylamine (BZA) and doxorubicin (DOX). Compared with an ordered block structure, random grafting of DIP, BZA and DOX is theoretically favourable for the formation of vesicle membrane with uniform microstructure. In our polymer design, conjugation of DOX through disulfide bonds makes the polymer reduction-sensitive, and grafting DIP endows the polymer with pH sensitivity which turns the hydrophobic block of PAsp(DIP-co-BZA-co-DOX) to be more hydrophilic following the pH change from neutral to acidic.³⁸ Furthermore, the π - π interaction enhanced hydrophobic interaction of the BZA groups was also thought to prevent micelle dissociation.³⁹ The polymers were characterized by ¹H NMR, gel permeation chromatography (GPC), and Raman spectral analyses.

Based on the integral values of characteristic peaks detected by ¹H NMR measurements, the grafting degrees of DIP, BZA and DOX in each polymer chain were 45, 5 and 8, respectively (Fig. S2). According to its grafting degree, DOX accounts for 21.52% (weight percentage) in the copolymer. All copolymers showed a unimodal molecular weight distribution in their GPC chromatograms indicating ideal purity (Fig. S3). The molecular weights of the copolymers obtained in ¹H NMR and GPC measurements were listed in Table S1.

Vesicles were prepared based on PDBD at pH 7.4 using the double emulsion method. The loading contents of chemically conjugated DOX, physically encapsulated DOX and arsenite ion in the D-As-PDBD vesicle were 21.52%, 4.20% and 2.04%, respectively. The physical encapsulation of the two hydrophilic therapeutic agents into the aqueous lumen of the vesicle only resulted in very slight size increase of the vesicle at pH 7.4, i.e. 182 ±5 nm of D-As-PDBD vesicle vs 173 ±4 nm of PDBD vesicle (Table 1). D-As-PDBD vesicle possessed uniform particle size and spherical morphology at pH 7.4 (Fig. 2A). Owing to dual-sensitive structural design of vesicle, decrease of the solution pH and addition of reducing agent GSH affected the particle size and morphology,

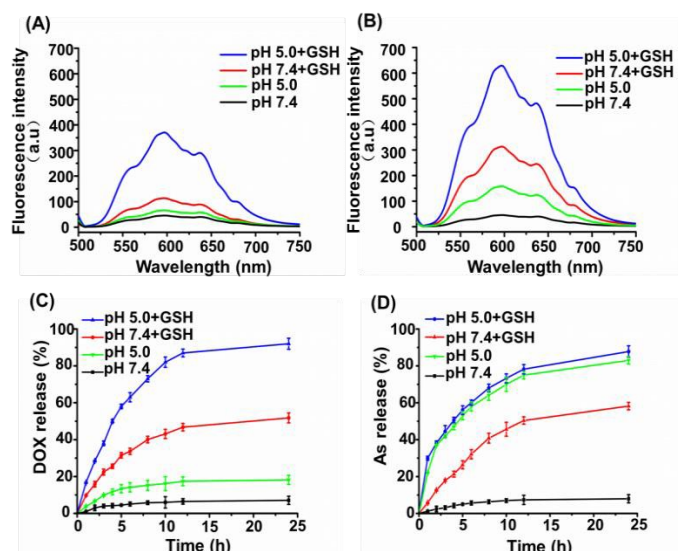


Fig. 3. DOX fluorescence intensities of PDBD vesicle (A) and D-As-PDBD vesicle (B) in aqueous solutions. In vitro DOX release (C) and As release (D) from D-As-PDBD vesicle in PBS. GSH concentrations if applied: 10 mM; study performed at 37°C; data were mean \pm SE (n =3); PDBD vesicle only carried conjugated DOX; D-As-PDBD vesicle carried chemically conjugated DOX, physically entrapped water-soluble DOX and As.

shown in TEM and DLS measurements (Fig. 2B-C and Table 1). When 10 mM GSH was present in the solution, the vesicle expanded to 210 ± 7 nm from 182 ± 5 nm, due to the breakage of disulfide bonds which led to the release of conjugated DOX and thereby decrease of the vesicle membrane hydrophobicity. At pH 5.0, the hydrophobic/hydrophilic ratio of mPEG-PAsp(DIP-co-BZA-co-DOX) decreased significantly due to the protonation of the DIP groups. As a result, the vesicle structure was destroyed and meanwhile micelle with much smaller size (35 ± 2 nm) was formed based on the hydrophobic interactions of the remained hydrophobic moieties such as the conjugated DOX and BZA groups. Moreover, nanoparticle was undetectable by DLS measurement in the solution of pH 5.0 plus 10 mM GSH, indicating complete vesicle dissociation. Consequently, drying the solution for TEM measurement formed random polymer aggregates (Fig 2D). These results evidenced the pH and reduction dual-sensitivity of D-As-PDBD vesicle, which was expected to facilitate an intracellular drug release. The D-As-PDBD vesicle showed good serum stability in aqueous solution. No obvious change in particle size was detected in the prolonged experimental time of 96 h when 10% fetal bovine serum (FBS) was present in the vesicle solution (Fig. S5).

Reduction and pH-sensitive drug release

The dual-sensitive drug release behaviour of the PDBD vesicle and

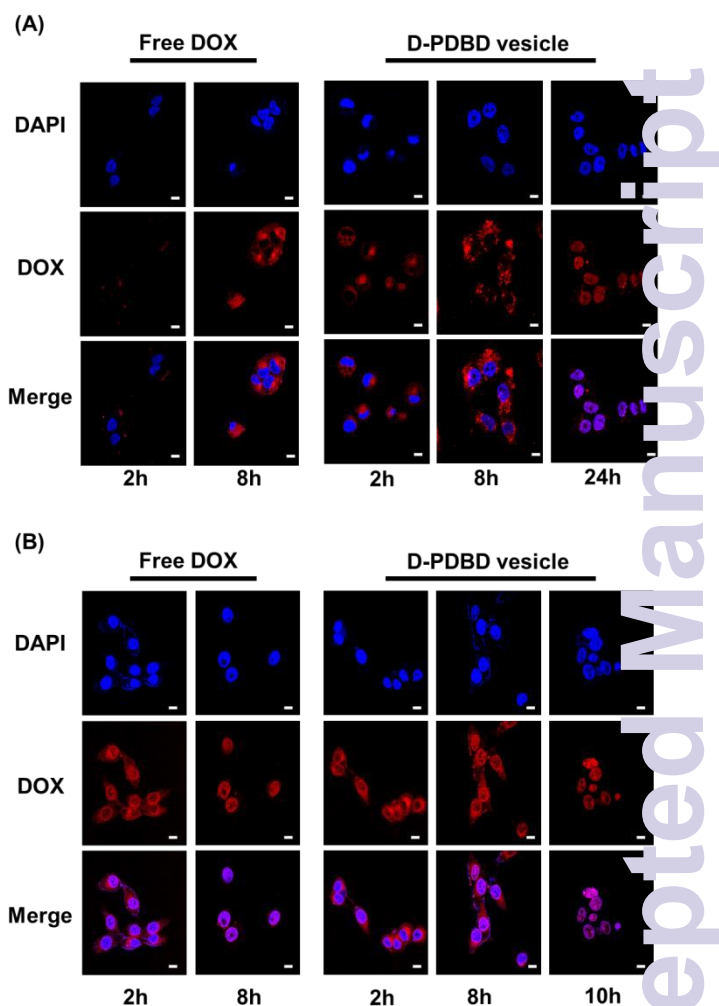


Fig. 4. Confocal Laser Scanning Microscopy (CLSM) images of MCF-7/ADR cells (A) and MCF-7 cells (B) incubated with free DOX and D-PDBD vesicle at different time points (DOX concentrations: 10 μ g/mL). Red fluorescence: DOX; blue fluorescence: nuclei stained with DAPI. The scale bars represent 10 μ m.

D-As-PDBD vesicle was verified *in vitro* by measuring the fluorescence intensities of DOX in the vesicle solution at various conditions. The DOX fluorescence intensity of PDBD vesicle was very low at pH 7.4 in the absence of GSH due to the fluorescence quenching effect of aggregated DOX (Fig. 3A). Compared to the solution pH change to 5, addition of 10 mM GSH increased the DOX fluorescence intensity of PDBD vesicle solution more effectively. Moreover, at the dual stimulations of pH 5.0 and 10 mM GSH, the DOX fluorescence intensity of PDBD vesicle solution increased most significantly, since in this condition the vesicle was completely dissociated to easily release DOX cleaved from the polymer as demonstrated in the TEM and DLS measurement. Similar reduction and pH-sensitive DOX release behaviours were detected with the D-As-PDBD vesicle, except that solely decrease

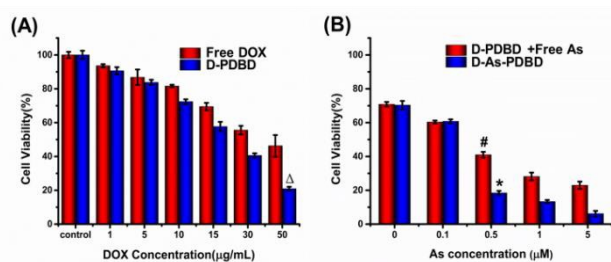


Fig. 5. MCF-7/ADR cytotoxicities of free DOX and D-PDBD vesicle relative to DOX concentration (A), and D-As-PDBD and D-PDBD + free As relative to As concentration (B). Data were detected by MTT assay (mean \pm SE; $n = 3$); DOX concentration in (B): 10 $\mu\text{g}/\text{mL}$. $^{\Delta}P < 0.05$ vs free DOX treatment group; $^{\#}P < 0.05$ vs D-PDBD treatment group without As; $^{*}P < 0.05$ vs D-PDBD + Free As treatment group.

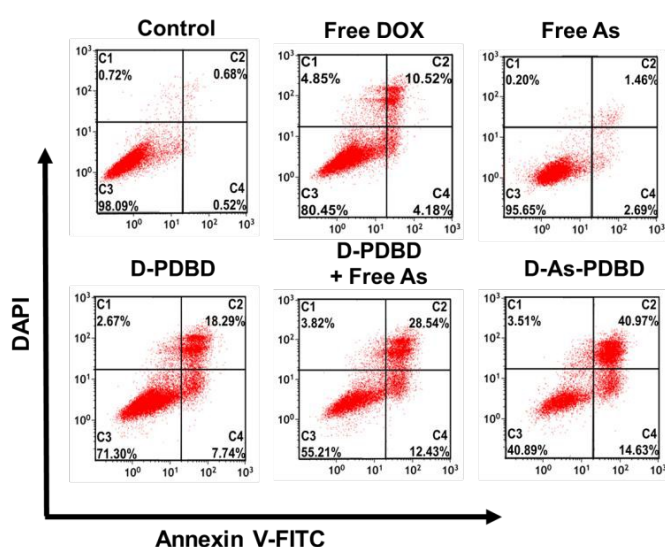


Fig. 6. Detection of apoptotic MCF-7/ADR cells using Annexin V-FITC and DAPI flow cytometry assay at various cell culture conditions. C1: necrotic cells; C2: late stage apoptotic cells; C3: normal viable cells; C4: early stage apoptotic cells; DOX concentration if applied: 10 $\mu\text{g}/\text{mL}$; As concentration if applied: 0.5 μM .

the solution pH to 5.0 appeared to increase the DOX fluorescence intensity more remarkably (Fig. 3B). This result was in line with the TEM observation that the vesicle structure was destroyed and the polymer reassembled into micelle structure at pH 5.0. Apparently, release of the free DOX molecules physically encapsulated inside the aqueous core rather than the chemically conjugated DOX inside the membrane of the D-As-PDBD vesicle has resulted in the appreciable increase of DOX fluorescence intensity at pH 5.0 without GSH addition.

Quantitative determination of DOX and As release from the D-As-PDBD vesicle was further conducted, which obtained consistent

results. As shown in Fig. 3C and D, release of DOX and As was both accelerated at pH 7.4 plus 10 mM GSH. Moreover, both drugs were released most rapidly at dual stimulations (pH 5.0 plus 10 mM GSH), due to the complete dissociation and cleavage of conjugated DOX. Notably, at pH 5.0 without addition of GSH, the As release was much more quickly than DOX release because the chemically conjugated DOX could not be released in this condition.

Cell uptake and intracellular distribution

Cell uptake and intracellular distribution of D-PDBD vesicle and free DOX were evaluated by confocal laser scanning microscopy (CLSM) in MCF-7/ADR and MCF-7 cells. As shown in Fig. 4, MCF-7 and MCF-7/ADR cells behaved much different in taking up free DOX. Free DOX entered MCF-7 cells and then migrated into nuclei quickly. In MCF-7/ADR cells, cell uptake level of DOX was much lower than that in the MCF-7 cells at the same incubation time points such as 2 h, apparently due to the drug efflux effect. Moreover, even after 8 h, free DOX still did not accumulate in nuclei. Compared to free DOX, the D-PDBD vesicle can effectively enter both the MCF-7 and MCF-7/ADR cells. Although slower and less compared to MCF-7 cells, nucleic accumulation of DOX in MCF-7/ADR cells still completed within 24 h, indicating that DOX was effectively released from the vesicle and then migrated to nuclei in both cells. These results are consistent with previous reports that nanomedicines may bypass the drug efflux pump,⁶⁻⁹ and we demonstrated that our dual sensitive design of the vesicle has led to the quick intracellular drug release.

Cytotoxicity assay

DOX is a well-known anticancer drug for the treatment of various cancers, and arsenite (As) has been recognized as a successful anticancer agent for acute promyelocytic leukemia (APL) therapy.²²⁻²⁴ The cytotoxicities of free As and DOX in MCF-7 cells and drug resistant strain MCF-7/ADR cells were evaluated with MTT assay. As shown in Fig. S6A, MCF-7 cells were sensitive to free DOX even at fairly low DOX concentrations such as 5 $\mu\text{g}/\text{mL}$. In contrast, the MCF-7/ADR cells were much less sensitive to DOX treatment. For example, more than 80% MCF-7/ADR cells were still viable at the DOX concentration of 10 $\mu\text{g}/\text{mL}$. Meanwhile, MCF-7/ADR cells appeared obviously less sensitive to As treatment than MCF-7 cells as well in terms of cytotoxicity. At the low As concentration below 1 μM , free As was almost non-cytotoxic to MCF-7/ADR cells (Fig. S6B). In contrast, free As below 1 μM was

still effectively suppress the growth of MCF-7 cells. DOX delivery using vesicle showed certain effect on circumventing the drug efflux pumps. Although D-PDBD and free DOX did not show obvious difference in suppressing the MCF-7/ADR cell growth at low DOX concentrations, at high DOX concentrations ranging from 10 to 50 $\mu\text{g/mL}$, the D-PDBD vesicle was more effective in decreasing the viability of MCF-7/ADR cells compared to free DOX (Fig. 5A). For example, the cell viabilities for D-PDBD vesicle and free DOX were 72.32% and 81.56% respectively at the DOX concentration of 10 $\mu\text{g/mL}$.

MCF-7/ADR cells were used to further verify the synergistic effect of As and DOX, as As has been found to suppress drug resistance of cancer cells through multiple mechanisms including down-regulation of the Bcl-2 and P-gp proteins.⁴⁰ The synergistic effect of As and DOX was evaluated in two different drug treatment approaches, i.e. one treatment using D-PDBD vesicle plus free As and another using DOX-As-co-loaded vesicle (D-As-PDBD vesicle). As shown in Fig. 5B, the effect of D-PDBD vesicle in suppressing MCF-7/ADR cell growth may be improved when a low concentration of free As was present in the cell culture medium. As free arsenite was almost non-cytotoxic to MCF-7/ADR cells at concentration below 1 μM , the above result implies that As might increase the chemotherapeutic effect of DOX *via* a synergistic manner. Moreover, compared to D-PDBD plus free As, the D-As-

PDBD vesicle appeared even more potent in inducing cell death, likely due to the fact that the vesicle-transported As circumvented the efflux pump (Fig. 5B)

Cell apoptosis

Annexin FITC/DAPI assay was conducted to reveal whether the above mentioned synergetic actions of As and DOX on MCF-7/ADR cells may result in enhancement of cell apoptosis. As shown in Fig. 6, no obvious apoptosis were detected when cells were treated with free DOX at 10 $\mu\text{g/mL}$ and free As at 0.5 μM . In comparison, DOX delivered by D-PDBD vesicle exerted better pro-apoptosis effect, leading to 26.03% apoptotic cells. The percentage of apoptotic cells further increased to 40.97% when D-PDBD vesicle was used in combination with free As. More excitingly, the apoptosis-inducing effect of D-As-PDBD vesicle was even much better than that of D-PDBD vesicle plus free As (55.60% vs 40.97%).

The TUNEL assay also confirmed the synergistic effect of two therapeutic agents co-delivered by the D-As-PDBD vesicle. As shown in Fig. S8, the nuclei of the apoptotic cells was stained brown, and no evident cell apoptosis was observed in the MCF-7/ADR cells treated with single drug, i.e. free DOX, free As or DOX delivered with D-PDBD vesicle. However, the percentages of apoptotic cells in the D-PDBD vesicle plus free As treatment and D-As-PDBD vesicle treatment were remarkably increased up to 45.04% and 62.17%, respectively.

Drug resistant gene expressions in MCF-7/ADR cells under various treatments

The mRNA and protein expression levels in the combined therapy of As and DOX were detected. Compared with PBS treatment, a single DOX treatment (10 $\mu\text{g/mL}$) using free DOX and D-PDBD vesicle in MCF-7/ADR cells significantly up-regulated Bcl-2 gene expression up to 248.60% and 159.82% respectively (Fig. 7), which indicated that the vesicle form of DOX somewhat reduced the elevated level of Bcl-2 in the drug-resistant cell. A similar trend of P-gp gene expression was also observed when MCF-7/ADR cells treated with different forms of DOX. Free DOX and D-PDBD vesicles up-regulated the P-gp gene expression by 239.58% and 140.67% respectively, at the DOX concentration of 10 $\mu\text{g/mL}$. Free As at various concentrations showed the activity to reduce the expression of P-gp and Bcl-2 genes. Nevertheless, free As above 1 μM resulted in a recovery of the expressions of the two drug resistant genes to some extent (Fig. S7). These results are in line with that of our

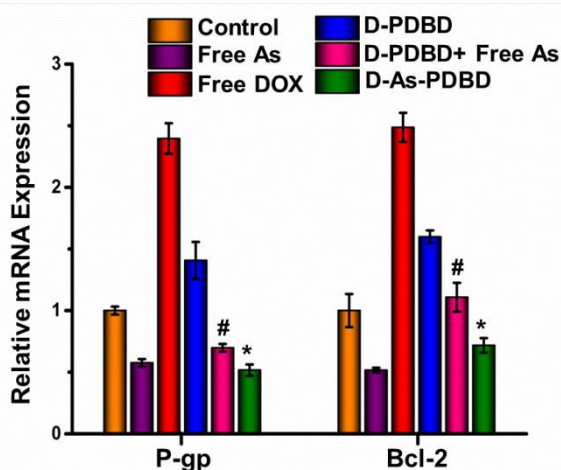


Fig. 7. The suppression of P-gp and Bcl-2 gene with different treatments in MCF-7/ADR cells evaluated at mRNA level by real-time PCR (mean \pm SE; n = 3). DOX concentration if applied: 10 $\mu\text{g/mL}$; As concentration if applied: 0.5 μM ; * P < 0.05 vs D-PDBD treatment group; # P < 0.05 vs D-PDBD treatment group.

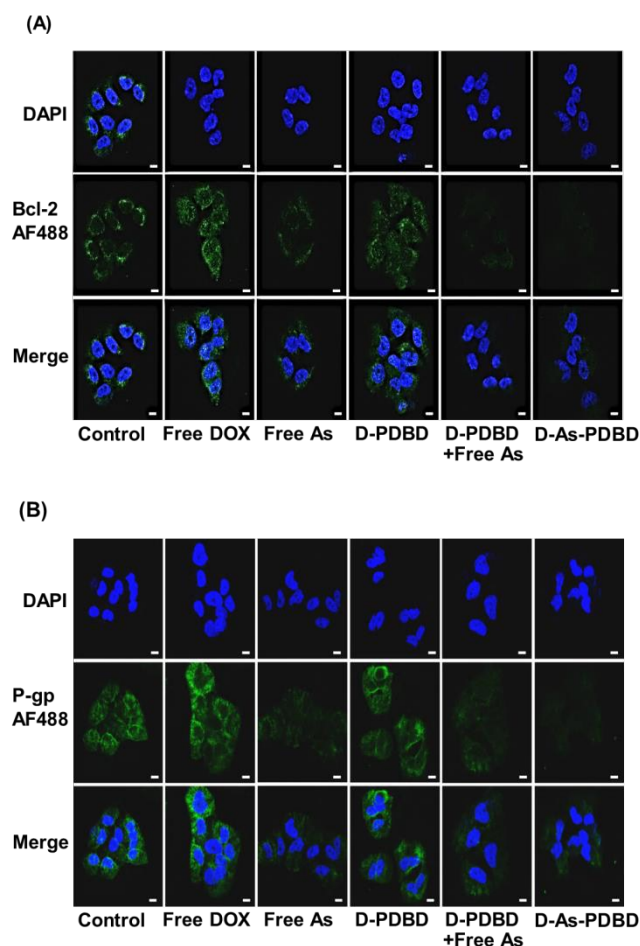


Fig. 8. Immunofluorescence images of MCF-7/ADR cells incubated different samples for Bcl-2 expression (A) and P-gp expression (B) in MCF-7/ADR cells. DOX concentration: 10 $\mu\text{g}/\text{mL}$; As concentration: 0.5 μM ; blue fluorescence: nuclei stained with DAPI; green fluorescence: Alexa Fluor[®] 488; scale bars: 10 μm .

studies.⁴¹⁻⁴³ Further study demonstrated the synergistic effect of DOX and As co-delivered with vesicle (Fig. 7). Compared to the D-PDBD treatment without As, the expression levels of P-gp and Bcl-2 in the D-PDBD vesicle plus free As group were down-regulated by 70.96% and 48.98%, respectively. Furthermore, the expression levels of P-gp and Bcl-2 in the D-As-PDBD vesicle group were more effectively down-regulated by 18.04% and 39.09%, respectively. The enhanced gene down-regulation effect in the D-As-PDBD vesicle group is likely due to the reduction of P-gp-mediated As efflux in the MCF-7/ADR cells.^{7, 8}

Evaluation of drug resistant gene expressions at protein level using an immunofluorescence assay was highly supportive of the above real-time PCR data. As shown in Fig 8, an obvious up-regulation of P-gp protein and Bcl-2 protein was found in the free DOX and D-PDBD vesicle treatment groups. Free As present in the

cell culture medium suppressed the up-regulation of the drug resistant genes induced by the D-PDBD vesicle treatment. Such As-induced target gene down-regulation was further punctuated when the cells were treated with D-As-PDBD, as shown by the further decreased green fluorescence reflecting the contents of P-gp and Bcl-2 proteins.

Conclusion

A novel reduction and pH dual-sensitive diblock copolymer mPEG-PAsp(DIP-co-BZA-co-DOX) (PDBD) was synthesized. In aqueous media, the copolymer self-assembled into a vesicle carrying chemically conjugated DOX in its dual-sensitive hydrophobic membrane and water-soluble DOX.HCl/arsenite in its aqueous core. The drug loading strategy combining chemical conjugation and physical entrapment achieved a high DOX loading in the vesicles (Total DOX loading: 25.72%). Meanwhile, the dual-sensitive structure design of vesicle allowed a quick intracellular drug release in response to the microenvironments inside cancer cells. *In vitro* biological experiments clearly showed that the co-delivered DOX and As exerted synergistic effects in inducing apoptosis and suppressing growth of the drug resistant breast cancer cells (MCF-7/ADR) *via* combined mechanisms. That is, As suppressed the DOX treatment-induced overexpression of anti-apoptotic gene (Bcl-2), and the small molecular drugs may bypass the P-gp efflux pump when they were transported into cancer cells with nanocarriers. The DOX and As co-delivery using the reduction and pH dual-sensitive vesicle may represent a new treatment modality for chemotherapy of drug resistant breast cancer.

Acknowledgements

This work was supported by National Basic Research Program of China (2015CB755500), the National Natural Science Foundation of China (51225305, U1401242, 51373203 and 21174166) and Natural Science Foundation of the Guangdong Province (2014A030312019, S2012020011070), the Guangdong Innovative and Entrepreneurial Research Team Program (2013S086).

References

1. M. E. Davis, Z. G. Chen and D. M. Shin, *Nature Reviews Drug Discovery*, 2008, **7**, 771-782.
2. M. Motornov, Y. Roiter, I. Tokarev and S. Minko, *Progress in Polymer Science*, 2010, **35**, 174-211.
3. H. Lee, E. Lee, D. K. Kim, N. K. Jang, Y. Y. JeonG and S. Jon, *J. Am. Chem. Soc.*, 2006, **128**, 7383-7389

4. J. Yang, T.-I. Lee, J. Lee, E.-K. Lim, W. Hyung, C.-H. Lee, Y. J. Song, J.-S. Suh, H.-G. Yoon and Y.-M. Huh, *Chemistry of Materials*, 2007, **19**, 3870-3876.
5. A. Marin, H. Sun, G. Hussein, W. Pitt, D. Christensen and N. Rapoport, *Journal of Controlled Release*, 2002, **84**, 39-47.
6. A. Kabanov, E. Batrakova and V. Alakhov, *Advanced Drug Delivery Reviews*, 2002, **54**, 759-779.
7. E. S. Lee, K. Na and Y. H. Bae, *Journal of Controlled Release*, 2005, **103**, 405-418.
8. C. Vauthier, C. Dubernet, C. Chauvierre, I. Brigger and P. Couvreur, *Journal of Controlled Release*, 2003, **93**, 151-160.
9. F. Bai, C. Wang, Q. Lu, M. Zhao, F.-Q. Ban, D.-H. Yu, Y.-Y. Guan, X. Luan, Y.-R. Liu and H.-Z. Chen, *Biomaterials*, 2013, **34**, 6163-6174.
10. Y. Shen, E. Jin, B. Zhang, C. J. Murphy, M. Sui, J. Zhao, J. Wang, J. Tang, M. Fan and E. Van Kirk, *Journal of The American Chemical Society*, 2010, **132**, 4259-4265.
11. B. Romberg, W. E. Hennink and G. Storm, *Pharmaceutical Research*, 2008, **25**, 55-71.
12. X. Guo, C. Shi, J. Wang, S. Di and S. Zhou, *Biomaterials*, 2013, **34**, 4544-4554.
13. H. Yoo, E. Lee and T. Park, *Journal of Controlled Release*, 2002, **82**, 17-27.
14. Y. Bae, S. Fukushima, A. Harada and K. Kataoka, *Angewandte Chemie-international Edition*, 2003, **42**, 4640-4643.
15. X. Wang, G. Wu, C. Lu, W. Zhao, Y. Wang, Y. Fan, H. Gao and J. Ma, *European Journal of Pharmaceutical Sciences*, 2012, **47**, 256-264.
16. Y.-J. Gu, J. Cheng, C. W.-Y. Man, W.-T. Wong and S. H. Cheng, *Nanomedicine-nanotechnology Biology And Medicine*, 2012, **8**, 204-211.
17. S. Yoon, W. J. Kim and H. S. Yoo, *Small*, 2013, **9**, 284-293.
18. M. H. Lee, Z. Yang, C. W. Lim, Y. H. Lee, S. Dongbang, C. Kang and J. S. Kim, *Chemical Reviews*, 2013, **113**, 5071-5109.
19. B. Khorsand, G. Lapointe, C. Brett and J. K. Oh, *Biomacromolecules*, 2013, **14**, 2103-2111.
20. Y. Hu, W. Yuan, N.-N. Zhao, J. Ma, W.-T. Yang and F.-J. Xu, *Biomaterials*, 2013, **34**, 5411-5422.
21. N. Zhao, X. Lin, Q. Zhang, Z. Ji and F.-J. Xu, *Small*, 2015, DOI: 10.1002/sml.201502760.
22. C. Qian, Y. Wang, Y. Chen, L. Zeng, Q. Zhang, X. Shuai and K. Huang, *Biomaterials*, 2013, **34**, 6175-6184.
23. E. W. LaPensee and N. Ben-Jonathan, *Endocrine-related Cancer*, 2010, **17**, R91-R107.
24. W. Chen, Y. Yuan, D. Cheng, J. Chen, L. Wang and X. Shuai, *Small*, 2014, **10**, 2678-2687.
25. H. Wu, W. N. Hait and J.-M. Yang, *Cancer Research*, 2003, **63**, 1515-1519.
26. C. Nieth, A. Priebisch, A. Stege and H. Lage, *FEBS Letters*, 2003, **545**, 144-150.
27. E. Yague, C. F. Higgins and S. Raguz, *Gene Ther*, 2004, **11**, 1170-1174.
28. A. Stege, A. Priebisch, C. Nieth and H. Lage, *Cancer Gene Ther*, 2004, **11**, 699-706.
29. Z. Duan, K. A. Brakora and M. V. Seiden, *Molecular Cancer Therapeutics*, 2004, **3**, 833-838.
30. X.-B. Xiong and A. Lavasanifar, *ACS Nano*, 2011, **5**, 5202-5213.
31. A. L. Jackson and P. S. Linsley, *Trends in Genetics*, 2004, **20**, 521-524.
32. G. Baj, A. Arnulfo, S. Deaglio, R. Mallone, A. Vigone, M. G. D. Cesaris, N. Surico, F. Malavasi and E. Ferrero, *Breast Cancer Research And Treatment*, 2002, **73**, 61-73.
33. A. Lemarie, C. Morzadec, D. Me'riano, O. Micheau, O. Fardel and L. Vernhet, *Journal of Pharmacology And Experimental Therapeutics*, 2006, **316**, 304-314.
34. S. Gupta, L. Yel, D. Kim, C. Kim, S. Chiplunkar and S. Gollapudi, *Molecular Cancer Therapeutics*, 2003, **2**, 711-719.
35. J. Li, T. Wang, D. Wu, X. Zhang, J. Yan, S. Du, Y. Guo, J. Wang and A. Zhang, *Biomacromolecules*, 2008, **9**, 2670-2676.
36. Y. Wang, E. Goethals and F. Du Prez, *Macromolecular Chemistry And Physics*, 2004, **205**, 1774-1781.
37. M. F. Zambaux, F. Bonneaux, R. Gref, P. Maincent, Dellacherie, M. J. Alonso, P. Labrude and C. Vigneron, *Journal of Controlled Release* 1998, **50**, 31-40.
38. M. Nakanishi, J.-S. Park, W.-D. Jang, M. Oba and K. Kataoka, *Reactive & Functional Polymers*, 2007, **67**, 1361-1372.
39. E. S. Lee, D. Kim, Y. S. Youn, K. T. Oh and Y. H. Bae, *Angewandte Chemie-international Edition*, 2008, **47**, 2418-2421.
40. A. L. Z. Lee, Y. Wang, H. Y. Cheng, S. Pervaiz and Y. Y. Yang, *Biomaterials Science*, 2009, **30**, 919-927.
41. D. Zhao, Y. Jiang, X. Dong, Z. Liu, B. Qu, Y. Zhang, N. Ma and C. Han, *Biomedicine & Pharmacotherapy*, 2011, **65**, 354-358.
42. D. Wang, H. Wei, H. Zhao, C. Hao, Z. Min and J. ... *Pharmaceutical Research* 2005, **52**, 376-385.
43. K. G. Chen, J. C. Valencia, J.-P. Gillet, V. J. Hearing and M. ... Gottesman, *Pigment Cell & Melanoma Research*, 2009, **22**, 740-749.